SUPPLEMENTAL MATERIAL FOR:

Sprouty2 inhibitory activity on FGF-signaling is modulated by the protein kinase DYRK1A

Sergi Aranda, Mónica Alvarez, Silvia Turró, Ariadna Laguna and Susana de la Luna

Supplemental Figure Legends

Supplemental Fig. S1. The conserved cysteine-rich domain of Spry2 is necessary for the interaction with DYRK1A

(A) Results of yeast two-hybrid experiments performed with wild-type DYRK1A (WT) and a catalytically inactive DYRK1A (K-R) as baits. The preys were the Spry2 clone found in the original screening and different deletion mutants. DYRK1A and Spry2 deletion mutants are shown schematically: DYRK1A: NLS, nuclear localization signal; KINASE, kinase catalytic domain; PEST, PEST domain; His, histidine repeat; S/T, serine/threonine-rich domain. Spry2: SRD, serine-rich domain; CRD, cysteine-rich domain. The positive (+) or negative (-) results for the interaction measured in a β-galactosidase filter assay are indicated. (B) Schematic representation of the GST-fusion proteins used in the pull-down assays shown in (C): SRD, serine-rich domain; CRD, cysteine-rich domain. (C) Bacterially expressed recombinant unfused GST, GST-Spry2 full-length (FL), and the deletion mutants GST-Spry2-(1-164) and GST-Spry2-(1-255) were immobilized to glutathione-Sepharose beads and incubated with soluble extracts of cells expressing HA-DYRK1A protein. Both the cell extracts (input) and the pulled-down proteins were analyzed by Western blot with an anti-HA

antibody. The unfused GST and GST-fusion proteins were visualized on the nitrocellulose membrane by Pounceau red staining. While the deletion of the most carboxy-terminal 60 amino acids in Spry2 yielded a protein still able to pull-down DYRK1A, the interaction almost disappeared when the complete Spry2 CRD was deleted.

Supplemental Fig. S2. The histidine domain in DYRK1A is necessary and sufficient to interact with Spry2

(A) Results of the yeast two-hybrid experiments performed with the Spry2 clone found in the original screen as a prey and different deletion mutants of DYRK1A as baits. Spry2 and the DYRK1A deletion mutants are shown schematically: Spry2: SRD, serine-rich domain; CRD, cysteine-rich domain. DYRK1A: NLS, nuclear localization signal; KINASE, kinase catalytic domain; PEST, PEST domain; His, histidine repeat; S/T, serine/threonine-rich domain. The positive (+) or negative (-) results for the interaction measured in a β-galactosidase filter assay are indicated. (B) HEK-293T cells were transfected with the expression plasmid encoding Flag-Spry2 and with pHA-DYRK1A encoding either the wild type (WT), the kinase-dead mutant (K-R), or carboxy-terminal deletion mutants (1-616) and (1-588), as indicated. The scheme above shows the proteins used. At 48 h post-transfection cell lysates were subjected to immunoprecipitation with anti-Flag antibody. Both the lysates and the immunoprecipitates (IP) were analyzed by Western blot with the indicated antibodies. DYRK1A and Spry2 interaction is independent of the kinase activity of DYRK1A. Moreover, whereas a DYRK1A mutant protein lacking the C-terminal 138 amino acids

can still interact with Spry2, binding is completely lost when the deletion extends a further 28 amino acids to delete the polyhistidine repeat segment in the DYRK1A (1-588) mutant. (C) HEK-293T cells were transfected with pFlag-Spry2, pHA-DYRK1A and increasing amounts of a plasmid expressing the enhanced green florescent protein fused to the histidine tail domain of DYRK1A (GFP-Hrep). Cell lysates were subjected to immunoprecipitation with anti-Flag antibody. Both the lysates and the immunoprecipitates (IP) were analyzed by Western blot with the indicated antibodies. Binding of DYRK1A to Spry2 is efficiently competed by increasing amounts of co-expressed GFP-Hrep.

Supplemental Fig. S3. Immunostaining patterns for Sprouty2 in mouse adult brain

Spry2 expression was analyzed by immunostaining with an anti-Spry2 specific antibody in the forebrain (A-D), midbrain (E-F) and hindbrain (G-L). In the forebrain, Spry2 immunoreactivity was general and diffuse everywhere in the neuropile. Regions displaying higher expression included the olfactory bulb (A), the prelimibic (B), cingulate, piriform and entorhinal cortices, hypothalamic and thalamic nuclei (C), and the hippocampal formation (D). In the midbrain, Spry2 immunostaining was detected throughout the neuropile. Intense immunoreactivity was observed in nuclei from the periaqueductal region, as the oculomotor nuclei (E), and nuclei from the pontine region (F). In the hindbrain, the cerebellar cortex showed high Spry2 expression, stronger in the Purkinje cell layer than in the granular cell and molecular layers (G). Staining in the Purkinje cell layer was observed in cell nuclei and proximal

dendrites (K). In addition, intense immunostaining was observed in deep cerebellar nuclei, vestibular nuclei (H), and several nuclei from the medulla and the pons, including motor nuclei such as the facial nuclei (I) and nuclei from the reticular formation such as the inferior olive (J). Neurons from this nuclei displayed strong cytoplasmic immunostaining in the soma and proximal neurites (L). Labelling in A-L: *AO*, anterior olfactory nuclei; *EPl*, external plexiform layer; *GrO*, granular cell layer; *Mi*, mitral cell layer of the olfactory bulb; PrL, prelimic cortex; *VMH*, ventromedial hypothalamic nuclei; *3V*, third ventricle; *Or*, stratum oriens; *CA3*, pyramidal cell layers; *LMol*, stratum lacunosum-moleculare; *Mol*, molecular layer of the dentate gyrus; *3N*, oculomotor nuclei; *Aq*, *sylvius* aqueductus; *Pn*, pontine nuclei; *cp*, cerebral peduncle; *P*, Purkinje cell layer; *Gr*, granular cell layer; *ML*, molecular layer; *Ve*, vestibular nuclei; *4V*, fourth ventricle; *7N*, facial nuclei; *sp*, spinal efferent tracts; *LRt*, lateral reticular nucleus; *IOM*, inferior olive medial nucleus; *Pyx*, pyramidal decussation. Scale bars correspond to 200 μm in A-J; 60 μm in K; 100 μm in L.

Supplemental Fig. S4. DYRK1A phosphorylates Spry2

(A) HEK-293T cells were transfected with expression plasmids encoding Flag-Spry2 with or without HA-DYRK1A. Soluble extracts were incubated for 30 min at 30ºC (30ºC) with alkaline phosphatase (Psa, 400 u/ml), or with alkaline phosphatase plus sodium pyrophosphate (200 mM) as a phosphatase inhibitor (P + I). Phosphatase activity was stopped by addition of sodium pyrophosphate to the lysates at a final concentration of 25 mM and samples were processed to be analyzed by Western blot with anti-Flag antibody. Control means untreated extracts. The lower mobility bands

of Spry2 (indicated as Pi-Spry2) appearing when co-expressed with DYRK1A, disappear when the extracts are treated with phosphatase, suggesting that they are the result of phosphorylation events. (B) The recombinant protein GST-Spry2 full length (FL) and the deletion mutant GST-Spry2-(1-255) were expressed in bacteria and purified. The proteins were used as substrates in an *in vitro* kinase assay with purified GST-DYRK1A as the source of the kinase activity. The samples were resolved by SDS-PAGE and analyzed by autoradiography. (C) Amino acid sequence of human Spry2 in which the putative DYRK1A phosphorylation sites are indicated: TP/SP pairs are in orange; R at position -3 is in light blue, with the phosphorylatable residue in red. Purple line correspond to the region where DYRK1A phosphorylates Spry2, and orange line indicates the binding region to DYRK1A.

Supplemental Figure S1
Aranda *et al.*

A

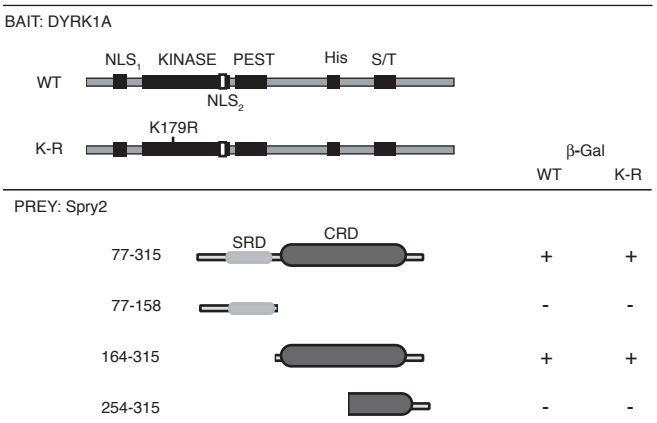

B

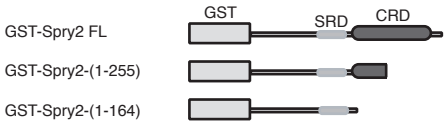

C

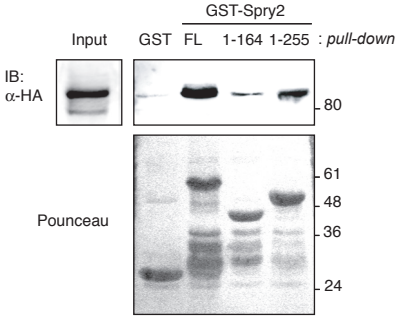

Supplemental Figure S2
Aranda *et al.*

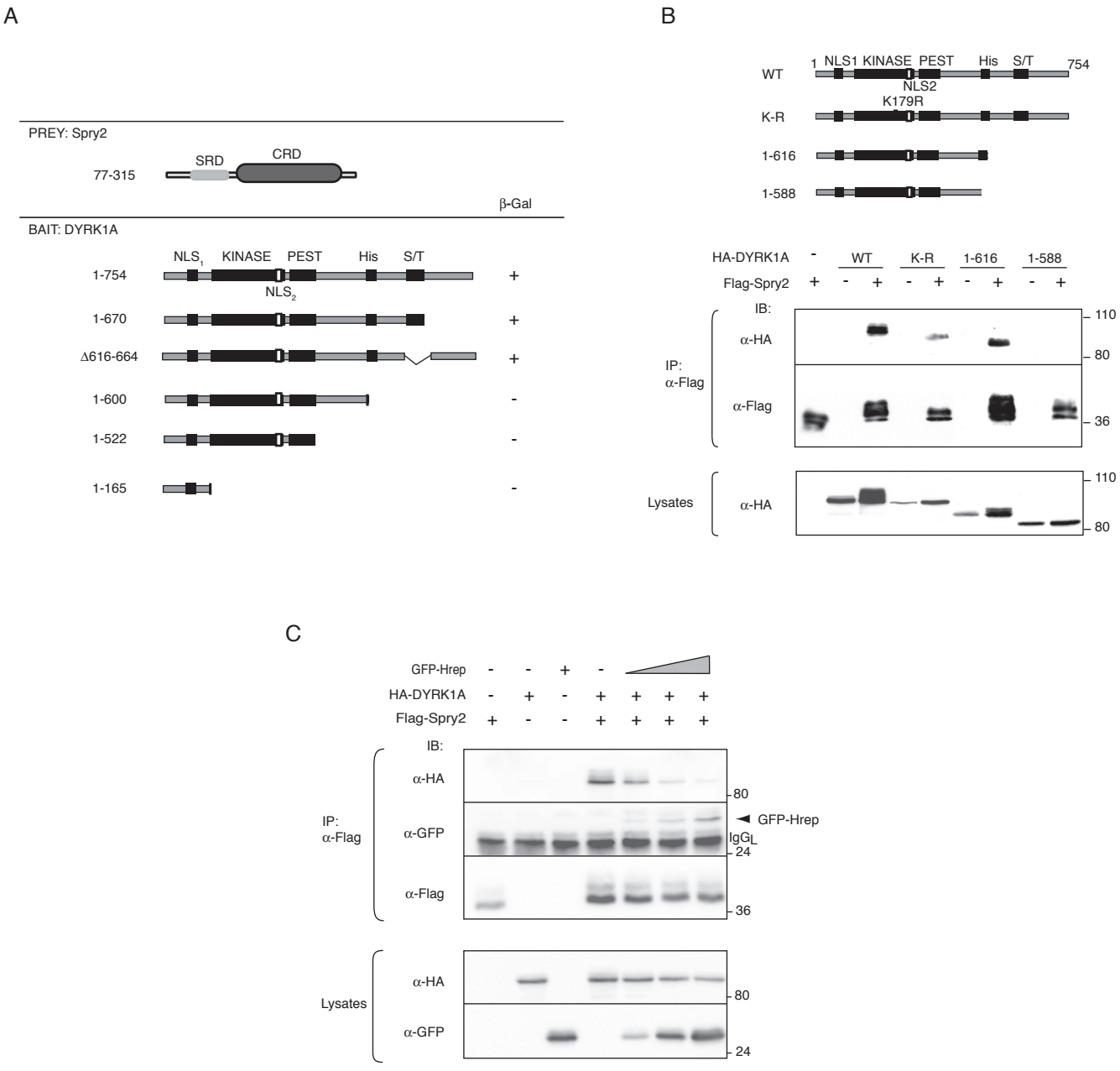

Supplemental Figure S3
Aranda *et al.*

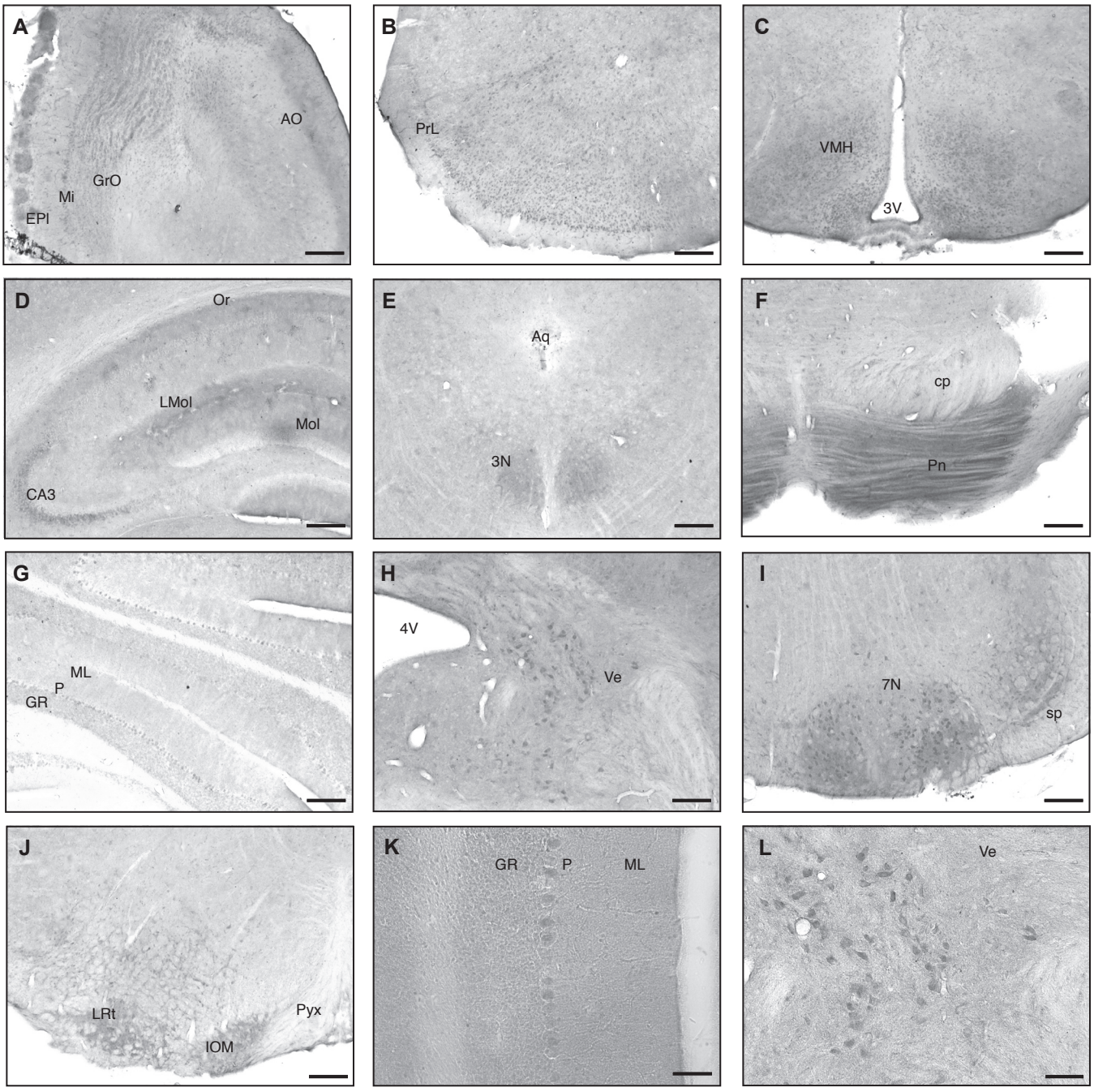

Supplemental Figure S4
Aranda *et al.*

A

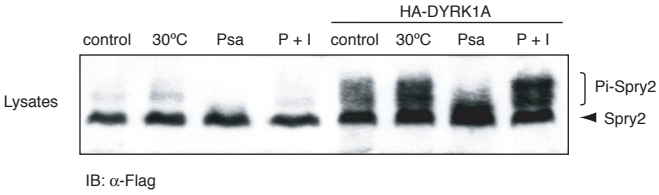

B

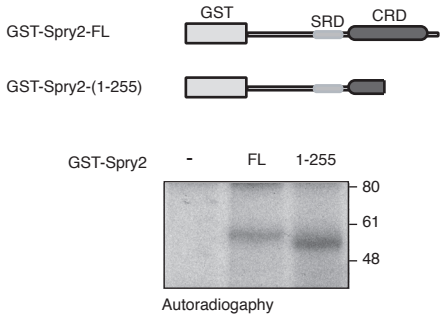

C

```
MEARASQGNGSQPLLQTPRDGGRQRGEPDPRDALTQQVHVLSLDQIRAIRNTNEYTEGPT  60
                *
VVPRPGLKPAPRPSTQHKHERLHGLPEHRQPPRLQHSQVHSSARAPLSRSISTVSSGSRS 120
                                                    164
STRTSTSSSSSEQRLLGSSFSSGPVADGIIRVQPKSELKPGELKPLSKEDLGLHAYRCED 180

CGKCKCKECTYPRPLPSDWICDKQCLCSAQNVIDYGTCVCCVKGLFYHCSNDDEDNCADN 240
                255
PCSCSQSHCCTRWSAMGVMSLFLPCLWCYLPAKGCLKLCQGCYDRVNRPGCRCKNSNTVC 300

CKVPTVPPRNFEKPT 315
```